Solar Activity Modeling: from Subgranular Dynamical Scales to the Solar Cycles

Irina N. Kitiashvili[1,2], Alan A. Wray[1], Viacheslav M. Sadykov[1,2], Alexander G. Kosovichev[1,3], Nagi N. Mansour[1]

[1]NASA Ames Research Center, [2]BAERI, [3]NJIT

The dynamical effects of solar magnetoconvection span a wide range spatial and temporal scales that extend from the interior to the corona and from fast turbulent motions to global magnetic activity. To study the solar activity on short temporal scales (from minutes to hours), we use 3D radiative MHD simulations that allow us to investigate complex tu interactions that drive various phenomena, such as plasma eruptions, spontaneous formation of magnetic structures, funnel-like structures and magnetic loops in the corona, and others. In particular, we focus on multi-scale processes of energy exchange across layers of the solar interior and atmosphere, which contribute to coronal heating and eruptive dynami modeling global-scale activity, we use a data assimilation approach that has demonstrated great potential for building reliable long-term forecasts of solar activity. In particular, it has been shown that the Ensemble Kalman Filter (EnKF) method applied to the Parker-Kleeorin-Ruzmaikin dynamo model is capable of predicting solar activity up to one sunspot cycle al time, as well as estimating the properties of the next cycle a few years before it begins. In this presentation, using the available magnetogram data, we discuss development of the methodology and forecast quality criteria (including forecast uncertainties and sources of errors). We demonstrate the influence of observational limitations on prediction accuracy, present the EnKF predictions of the upcoming Solar Cycle (25) based on both the sunspot number series and observed magnetic fields and discuss the uncertainties and potential of the data assimilation approach for modeling and forecasting solar activity.

'StellarBox' code (Wray et al., 2018)

- ✓ 3D rectangular geometry
- ✓ Fully conservative, Fully compressible
- ✓ Fully coupled radiation solver:
  - LTE using 4 opacity-distribution-function bins
  - Ray-tracing transport by Feautrier method
  - 18 ray angular quadrature
- ✓ Non-ideal (tabular) EOS
- ✓ 4th order Padé spatial discretization
- ✓ 4th order Runge-Kutta time integration
- ✓ Turbulence models:
  - Compressible Smagorinsky model
  - Compressible Dynamics Smagorinsky mode (Germano et al., 1991; Moin et al., 1991)
  - MHD subgrid models (Balarac et al., 2010)
  - DNS+Hyperviscosity approach
- ✓ MPI parallelization (plane and pencil versions)

Flow eruptions

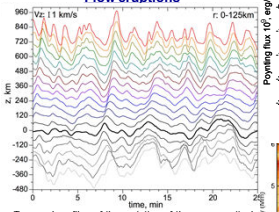

Temporal profiles of the variation of the mean vertical velocity in a vortex core, at different levels below the surface and in the atmosphere. The thick black curve shows the variation at the photosphere layer. The height difference between the curves is 60 km.

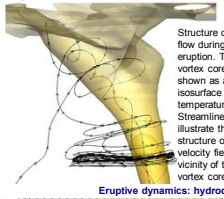

Structure of the flow during the eruption. The vortex core is shown as an isosurface of temperature. Streamlines illustrate the structure of the velocity field in the vicinity of the vortex core.

Eruptive dynamics: hydrodynamic vs magnetic forces

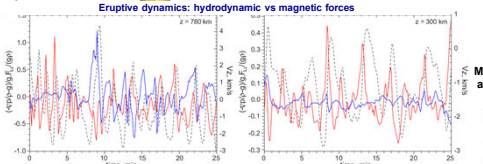

Magnetic field distribution at the photosphere

Magnetic structures formed by a turbulent dynamo on the Sun, generated from an initial random seed field. The blue-red color scale corresponds to magnetic field strength from -300 to 300 Gauss. The typical size of the magnetic structures is 100 to 300 km.

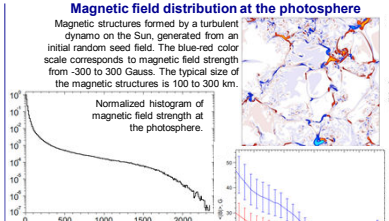

Mean vertical profiles of the unsigne magnetic field components.

Mean vertical Poynting flux as function of depth. Error bars how the standard deviation.

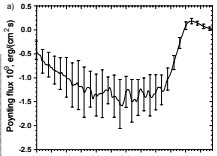

Modeling of self-organization processes in the solar corona

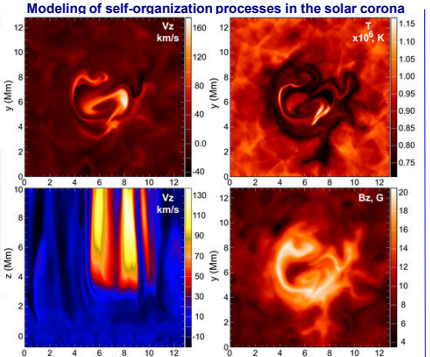

Variation of the turbulent magnetic Prandtl number from the subsurface to the corona

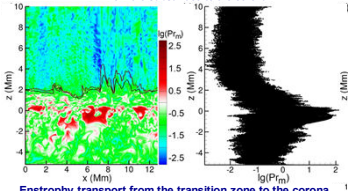

Temperature distribution in the magnetized solar corona

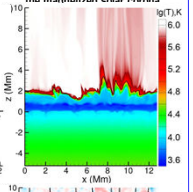

vertical velocity | magnetic field strength

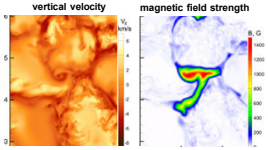

Log(Pmag) | magnetic diffusivity

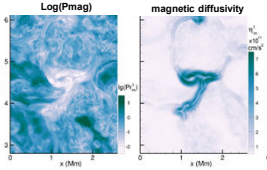

Enstrophy transport from the transition zone to the corona

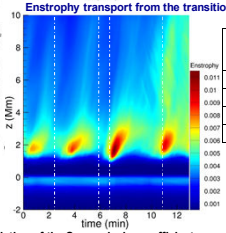

# Eruption	Enstrophy transport speed, km/s	
1	16	110
2	16	76
3	30	79
4	35	115

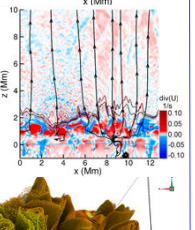

Mean variation of the Smagorinsky coefficients as a function of depth from the subsurface layers up to 20Mm high in the corona

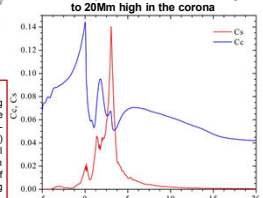

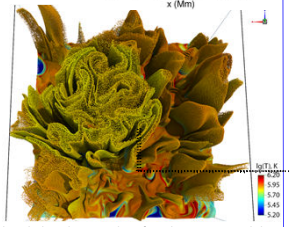

View through the solar atmosphere from the corona toward the transition zone and corona. The simulation results show a self-formed magnetic structure in the corona that is connected with kilogauss magnetic field in the photosphere through the chromosphere and transition zone. Visualization is performed by advecting particles seeded at height 2.4Mm above the solar surface. Credit T. Sandstrom

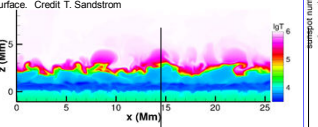

Conclusions I

To investigate the underlying physical processes, we performed 3D radiative MHD simulations, taking into account all essential physics and employing sub-grid scale turbulence models, and reproduce the local dynamo process, spontaneous flow eruptions, and coronal structure and dynamics in the quiet-Sun. The simulations revealed three important properties of the dynamo-generated magnetic fields: 1) strong coupling of various magnetic field amplification mechanisms, which leads to increased local magnetic energy, 2) the multi-scale nature of the dynamo process, which involves turbulent flows from the smallest resolved scales to granular scales, 3) a complex topological and dynamical structure of the process, which is reflected in the interaction of individual magnetic patches and surrounding magnetic fields and in the self-organization that produces a magnetic network.

Our simulations reveal penetration of vortex tubes from the photosphere into the corona. The vortex tube eruptions cause significant qualitative changes in atmospheric dynamics, such as strong variations in the thermodynamic structure, magnetic field-line topology, and local heating, and are also a source of local twisted upflows in the chromosphere. The plasma flow in the eruptions is accelerated by the Lorentz force from 6 to 12−15 km/s in higher (mid-chromospheric) layers.

Using an advanced 3D radiative MHD code, "StellarBox", we have performed the first high-resolution simulations of the Sun from the deep convection zone to the corona. It is found that the transition zone between the low temperature (10^4 K) chromosphere and hot (10^6 K) corona is substantially more turbulent and dynamic than previously assumed. The simulations revealed new processes of generation of shocks and plasma eruptions and showed that transition-region dynamics is a source of coronal expansion and formation of the solar wind.

References

Balarac G., Kosovichev A.G., Brugière O., Wray A.A., Mansour N.N., 2010. ArXiv: 1010.5759.
Evensen G. Data Assimilation. Springer. 2007.
Germano M., Piomelli U., Moin P., et al. 1991. Physics of Fluids **3**, p.1760.
Kitiashvili I.N. 2016. ApJ 831, article id. 15.
Kitiashvili I. N. & Kosovichev A. G. 2008. ApJ 688, L49-L52.
Kitiashvili I.N. & Kosovichev A.G. 2009. GAFD 103, 53-68.
Kitiashvili, I.N. & Kosovichev, A.G. 2011. Lecture Notes in Physics 832, p121.
Kitiashvili I.N. 2016. ApJ 831, article id. 15, 8 pp.
Kitiashvili I.N., 2019, eprint arXiv:1910.00820.
Kleeorin N.I., Ruzmaikin A.A. 1982. Magnetohydrodynamics, 18, 116.
Kleeorin N., Rogachevskii I., Ruzmaikin A. 1995. A&A 297, 159-167.
Moin P., Squires K., Cabot W., Lee, S., 1991. Physics of Fluids **3**, p.2746.

Data Assimilation Methodology

Observations

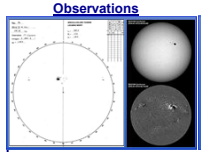

Dynamo model

$$\frac{\partial A}{\partial t} = \alpha B + \eta \nabla^2 A \qquad \alpha_k = -(\tau/3)\langle \mathbf{u}(\nabla \times \mathbf{u}) \rangle$$

$$\frac{\partial B}{\partial t} = G\frac{\partial A}{\partial z} + \eta \nabla^2 B \qquad \alpha_m = (\tau/12\pi\rho)\langle h(\nabla \times h) \rangle$$

$$\alpha = \alpha_k + \alpha_m$$

$$\frac{\partial \alpha_m}{\partial t} = \frac{\mu}{4\pi\rho}\left(\mathbf{B}\cdot(\nabla \times \mathbf{B}) - \frac{\alpha \mathbf{B}^2}{\eta}\right) - \frac{\alpha_m}{T_a}$$

Parker 1955, Kleeorin & Ruzmaikin, 1982, Kitiashvili & Kosovichev 2009

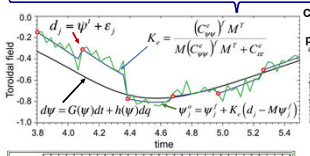

Comparison of sunspot number predictions and estimated parameters at the solar minima

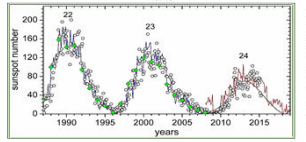

Comparison of the sunspot number prediction for Solar Cycle 24 (red curve, Kitiashvili & Kosovichev, 2008) and actual observations of monthly sunspot number. The blue curve shows the corrected dynamo solution according to annual sunspot number (green diamonds).

Vector-potential of the poloidal field changes sign corresponding to the polar field reversal. The amplitude at the start of Cycles 20 and 24 is substantially lower than during the other minima. The large-scale magnetic helicity shows significantly better correlation with future sunspot numbers; in particular, the magnetic helicity substantially decreases prior to weak sunspot cycles.

'Prediction' of Cycles 23 and 24 for both hemispheres using reconstructed toroidal and poloidal magnetic field co

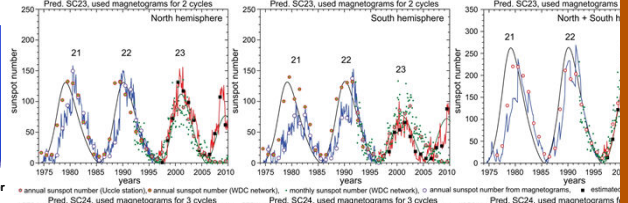

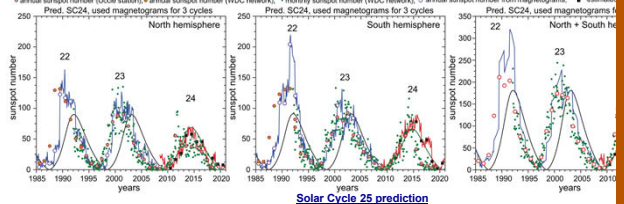

Solar Cycle 25 prediction

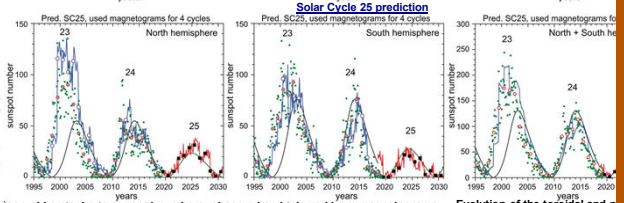

Synoptic magnetogram. The color scale is saturated at +/-15G. The yellow dashed lines indicate different moments of time: 1992 and 1994.

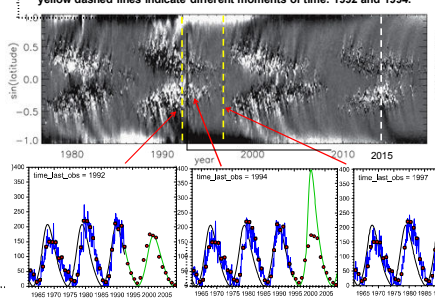

Comparison of hemispheric sunspot numbers, observed and interred from magnetograms

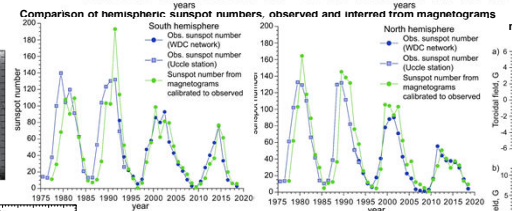

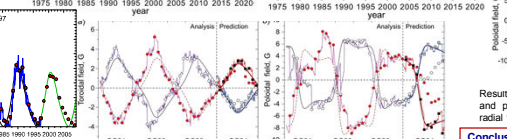

Evolution of the toroidal and p magnetic fields obtained from s magnetograms

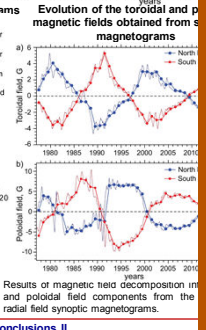

Results of magnetic field decomposition int and poloidal field components from the radial field synoptic magnetograms.

Uncertainties in Prediction of Solar Cycle 25 using sunspot number records

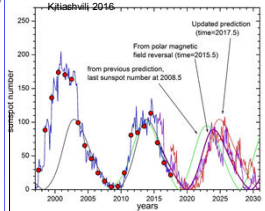

Early estimates of the properties of Solar Cycle 25 (for sunspot number version 2.0)

1) prediction obtained for observations which include the sunspot number data up to the solar minimum in 2008 (green curve);
2) prediction obtained for the last observation during polar magnetic field reversal (purple/violet curve);
3) prediction obtained using all currently available observations up to 2017 (red curve).

Blue curve shows the best EnKF estimates of the previous cycles based on the dynamo model and all available sunspot observations (red circles).

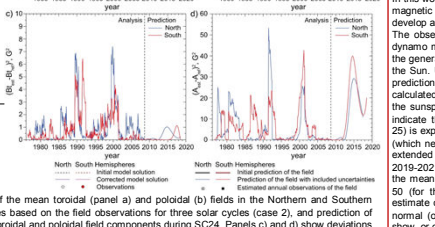

Evolution of the mean toroidal (panel a) and poloidal (b) fields in the Northern and Southern hemispheres based on the field observations for three solar cycles (case 2), and prediction of the mean toroidal and poloidal field components during SC24. Panels c) and d) show deviations of the model solutions for the magnetic field components from the observational data.

Conclusions II

In this work we take advantage of synoptic obse magnetic field emerging on the surface of t develop a more advanced and reliable forecasti The observational data are assimilated into a dynamo model which provides a theoretical de the generation and evolution of the global magr the Sun. Using the currently available observa predictions and prediction uncertainties h calculated for Solar Cycle 25. The results bas the sunspot number series and observed mag indicate that the upcoming Solar Maximum (25) is expected to be weaker than that of the c (which near its end). The model results show extended solar activity minimum is expecte 2019-2021, the maximum will occur in 2024 - the mean sunspot number at the maximum w 50 (for the v2.0 sunspot number series) wi estimate of ~15%. The maximum is likely to be normal (over 2 – 2.5-years), as the prediction show, or could exhibit a double hump structure.

The research is funded by the NSF SHINE program AGS-1622341 & NASA Heliophysics Support Program